Chemical Physics Letters 517 (2011) 92–97

Contents lists available at SciVerse ScienceDirect

Chemical Physics Letters

journal homepage: www.elsevier.com/locate/cplett

Derivation of diabatic potentials for F + H_2 employing non-adiabatic coupling terms

Anita Das [a], Debasis Mukhopadhyay [a,*], Satrajit Adhikari [b], Michael Baer [c]

[a] Department of Chemistry, University of Calcutta, Kolkata 700 009, India
[b] Department of Physical Chemistry, Indian Association for Cultivation of Science, Jadavpur, Kolkata 700 032, India
[c] The Fritz Haber Research Center for Molecular Dynamics, The Hebrew University of Jerusalem, Jerusalem 91904, Israel

ARTICLE INFO

Article history:
Received 16 March 2011
In final form 30 September 2011
Available online 8 October 2011

ABSTRACT

We present a study of the non-adiabatic coupling terms (NACTs) and the corresponding diabatic potentials for the reactive H_2 + F system in the entrance channel. The study reveals two conical intersections (*ci*): (I) A Jahn–Teller (1,2) *ci*, located at a point on the collinear HHF axis close to the minimum energy path; (II) A Renner–Teller *line* of (2,3) *cis*, along the collinear HHF axis. To form the *diabatic* potentials we consider only the two lower adiabatic potentials and the *quantized* Born–Oppenheimer mixing angles that guarantee *single-valued* diabatic potentials.

1. Introduction

The reactive (exchange) F + XY; X,Y = H,D systems have played an important role in the study of elementary chemical reactions for about half a century [1–19]. The number of Letters – experimental and theoretical – devoted to this reaction, exceeds the number of Letters related to any other single system in chemical physics. It is important to emphasize that the theoretical studies followed the outstanding experiments as were carried out during the last three decades of the last century by leading groups of Lee [1] in Berkeley, Polanyi and Woodall [2] in Toronto, Toennies [3] in Goettingen as well as by numerous other groups around the globe.

The most important requirement for a reliable *theoretical* study is having an *ab initio* potential energy surface (PES). The somewhat disappointing fact is that such a PES, to the best of our knowledge, does not exist for this system. The most that was done is calculating the *ab initio* adiabatic PESs [6] which suffice for a dynamic study within the Born–Oppenheimer (BO) approximation and revealing the existence of a conical intersection (*ci*) in the vicinity of the collinear minimum energy path [6]. Having the lowest adiabatic PES enabled a series of accurate dynamical treatments which yield results [3,7–12] that fit surprisingly well the experimental results just mentioned as well as many others.

The main reason for carrying out the present study is not so much to deliver a more up-to-date PES for the title reaction but to find out to what extent the *cis* of this system may affect the dynamics. To clarify what we have in mind we illuminate a recent important Letter by Lipoff and Herschbach (LH) [17] in which they distinguish between *Bare* and *Dressed* potentials (referring to the reactive F + H_2 system). Following this presentation the *Bare* PES is the one obtained from the electronic structure calculations (in other words, the lowest adiabatic PES) and the *Dressed* PES is the effective potential felt by the reactants when approaching each other at low temperatures (as encountered e.g. in Cold Reactions [13–15]). While doing this comparison LH showed that the potential barrier as well as the van-der-Waals potential well (both in the entrance channel) differ significantly due to these two numerical approaches.

Whereas LH used the lowest adiabatic PES to form the Dressed potential (see also Ref. [7]) the ultimate goal of our study is to calculate the Dressed potential applying *diabatic* potentials (based on BO potentials and BO NACTs). However since this seems, at this stage, to be a formidable task the present Letter is devoted to the methodology which eventually will enable us to calculate the diabatic potentials for the required three dimensional configuration space.

Two comments have to be made:

(i) It is important to mention that diabatic potentials were already calculated for this system [6] but these were derived in an approximate way ignoring the relevant BO NACTs. In contrast, the present treatment is more consistent [20,21] since it is based on BO NACTs that yield adiabatic-to-diabatic transformation (ADT) angles with *integer* Berry phases [22–25] which in turn guarantee *single-valued* diabatic potentials as required [26,27].

(ii) In contrast to recent treatments [e.g., 18,19] we did not include the spin–orbit (SO) coupling in our study. It is true that as long as this coupling is ignored the corresponding dynamic calculations cannot be really trusted. However once the methodology to form the diabatic potentials is fully developed the SO coupling will be included just as it is included in previous treatments.

* Corresponding author.
E-mail addresses: dm.chem.cu@gmail.com (D. Mukhopadhyay), michaelb@fh.huji.ac.il (M. Baer).

0009-2614/$ - see front matter © 2011 Elsevier B.V. All rights reserved.
doi:10.1016/j.cplett.2011.09.072

2. Background

To study the BO-NACTs and the positions of the corresponding conical intersections (*ci*), we consider a plane which contains the three atoms (A, B and C) where a point in configuration space (CS) is described in terms of three (Cartesian) coordinates (r,R,θ). Here r is the distance between two atoms (usually the atoms that form the diatomic molecule), R is a distance between the third atom and the center-of-mass of the diatom and θ is the angle between the two corresponding vectors **r** and **R**. In order to study the NACTs we break-up the three-dimensional CS and present it as a series of two-dimensional CSs which are chosen to be planes. Each plane is parameterized by a fixed value of r. This parameterization leaves, two of the three coordinates, R and θ, free to describe the position of the third atom, A, on that plane. Atom A serves as a *test* particle to examine the values of the NACTs, $\tau_{jk}(R,\theta|r)$ at a given series of grid points. Consequently atom A is allowed to move freely on that plane, whereas atoms B and C are fixed so that $r = R_{BC}$. It is important to mention that in order to obtain the NACTs for the complete three-dimensional CS the value of r has to be varied systematically along a given grid (see more on this issue in Section 4).

In the present Letter we limit our study to the two lower states of the F + H_2 system, i.e. $1^2A'$, $2^2A'$ (although in the future we intend, to extend this study to ADT angles based on three states [25]) and therefore consider only one (vectorial) NACT, namely, $\boldsymbol{\tau}_{12}(R,\theta|r)$ that couples these two states (in what follows we drop the indices so that $\boldsymbol{\tau}(R,\theta|r) \equiv \boldsymbol{\tau}_{12}(R,\theta|r)$. As is revealed in the present study (see also Ref. [6]), this NACT is formed by a *ci* which is located on the collinear (reagent) axis at a finite distance in-between the fluorine and the nearby hydrogen.

As is well known, the diabatic potentials $V_1(\mathbf{s})$, $V_2(\mathbf{s})$, $V_{12}(\mathbf{s})$ are derived employing the ADT angle, $\gamma(\mathbf{s}|\Gamma)$ (also, known as the *mixing* angle) which, enables the *diabatization* of the two-state systems [20,21]. The ADT angle is calculated via line-integrals of the form [21]: $\gamma(\mathbf{s}|\Gamma) = \int_{\mathbf{s}_0}^{\mathbf{s}} \tau(\mathbf{s}'|\Gamma)\cdot \mathbf{ds}'$ where the integration is carried out along a contour Γ located in the planar CS (the two points **s** and $\mathbf{s}_0$ are on Γ) and the *dot* stands for a scalar product. As is noticed the tangential component is the only component relevant for calculating the ADT angle, so that if Γ is a circular contour (not necessarily with respect to the above-defined (r,R,θ) coordinates) the equation for γ simplifies to become:

$$\gamma_{12}(\varphi|q) = \int_0^{\varphi} \tau_{\varphi 12}(\varphi'|q)d\varphi' \tag{1}$$

where τ_φ $(\varphi|q)/q$ is the corresponding *angular* component of the NACT with the operator, τ_φ defined as $\tau_\phi(\phi|q) = \langle\zeta_1(\phi|q)(\partial/\partial\phi)\zeta_2(\phi|q)\rangle$. The two functions $\zeta_j(\varphi|q)$; $j = 1,2$ are the eigenfunctions related to the two lower states, mentioned earlier, and q and φ are the relevant polar coordinates with regard to some point on the planar CS (see Figure 1). In other words the position of atom A, along the circular contour, Γ, is now described in terms of the polar coordinates (q,φ). The two systems of coordinates (q,φ) and (R,θ), for a given r-value, are connected via simple geometrical relations (see Figure 1).

Given the two adiabatic PESs $u_j(\varphi|q)$; $j = 1,2$, the corresponding diabatic potentials $V_1(\varphi|q)$, $V_2(\varphi|q)$, $V_{12}(\varphi|q)$, are derived from the following set of equations [26,27]:

$$\begin{aligned} V_1(\varphi|q) &= u_1(\varphi|q)\cos^2\gamma(\varphi|q) + u_2(\varphi|q)\sin^2\gamma(\varphi|q) \\ V_2(\varphi|q) &= u_1(\varphi|q)\sin^2\gamma(\varphi|q) + u_2(\varphi|q)\cos^2(\varphi|q) \\ V_{12}(\varphi|q) &= (1/2)(u_2(\varphi|q) - u_1(\varphi|q))\sin(2\gamma(\varphi|q)) \end{aligned} \tag{2}$$

where $\cos^2\gamma$ is given in Eq. (1). The transformation that yields the diabatic potentials is presented explicitly to show that in order to guarantee the single-valuedness of these potentials – a requirement frequently ignored in numerical studies – the angle $\gamma(\varphi|q)$ has to be quantized [23–25]. This difficulty (which usually is not always easy to treat) was overcome here employing *complementary* line integrals (see Appendix A).

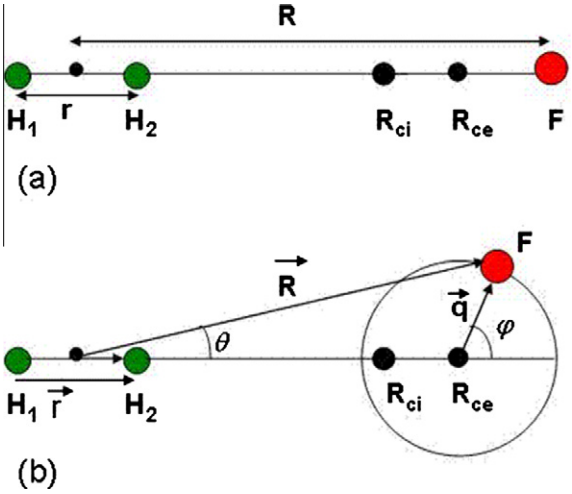

Figure 1. A schematic picture of the system of coordinates: (a) point of (1,2) *ci* (at R_{ci}), the center of all circular contours (at R_{ce}) and positions of atoms along the collinear axis. (b) System of coordinates: $(R,\theta|r)$ vs.$(\varphi,q|r)$. In this figure atoms F, H_1 and H_2 stand for atoms A, B and C, respectively, mentioned in the text.

3. Numerical results

The results to be reported in this Letter are obtained for configurations where the vibrational coordinate $r = R_{HH}$ is fixed and is equal to 1.6 au. The location of the Jahn–Teller (JT) (1,2) *ci* is revealed by *trial and error* and was found to be for the present case on the collinear axis at the vicinity of $R = R_{ci} \sim 5.5$ au.

As already mentioned earlier the numerical treatment is based on the explicit application of *ab initio* NACTs [20,21,28–39]. Consequently are considered four different types of results: (a) Angular NACTs (=$\tau_\varphi(\varphi|q)$); (b) Two-state ADT angles (=$\gamma(\varphi|q)$); (c) Adiabatic PESs (=$u_j(\varphi|q)$ $j = 1,2$); (d) The corresponding diabatic PESs, $V_1(\varphi|q)$ and $V_2(\varphi|q)$, and the diabatic coupling term $V_{12}(\varphi|q)$ (formed by employing Eqs. (2)). For the present study the *adiabatic* PESs and the corresponding NACTs were generated by applying MOLPRO [40] (see Appendix B for details).

As emphasized throughout this Letter the calculations are done along closed *circular* contours (to be able to guarantee the *single-valuedness* of the diabatic potentials). The radii of these circles are q and their centers are all located on the collinear axis at the same fixed point: $R = R_{ce} = 6$ au (thus removed, outward, by ~0.5 au from the position of the corresponding (1,2) *ci*-point – see Figure 1). This common center is chosen in such a way as to guarantee that the just mentioned circles cover the whole planar CS of interest.

As a final step are derived the two diabatic PESs: $V_1(R,\theta)$ and $V_2(R,\theta)$ and the corresponding coupling term $V_{12}(R,\theta)$ for a given *Cartesian* grid (R,θ) by performing the necessary transformations and interpolations.

In Figure 2 are presented the (1,2) NACTs, $\tau_\varphi(\varphi|q)$, for $q = 2.0$ au. The symmetric structure of the curve indicates that indeed $\tau_\varphi(\varphi|q)$ is formed by a *ci* located on the collinear axis showing two peaks, one due to NACTs mainly distributed along the $(\pi/2,\pi)$ sector and the other mainly along the $(\pi,3\pi/2)$ sector. The structure as a whole is tilted towards the HH axis. It is also well noticed that this NACT becomes negative along a short φ-interval which is usually a sign that it is affected by NACTs formed by higher states [30]. In our case the next possible NACT is a Renner–Teller (2, 3)

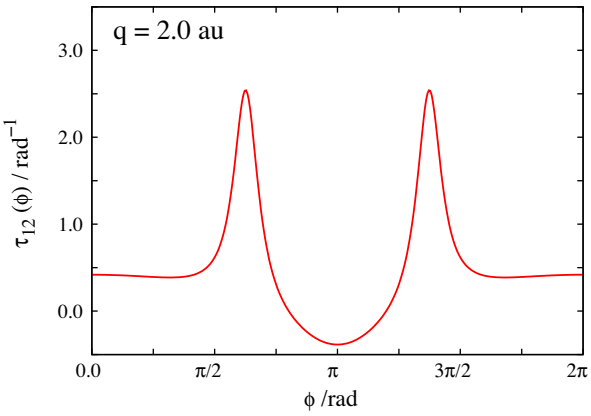

Figure 2. Angular NACTs. τ_{φ} $(\varphi|q = 2$ au), for circular contours at $R = R_{ce} = 6$ au along the interval $0 \leqslant \varphi \leqslant 2\pi$: Note that the left peak is located in the $\{\pi/2 \leqslant \varphi \leqslant \pi\}$ interval and the right peak is located in the symmetric interval: $\{\pi \leqslant \varphi \leqslant 3\pi/2\}$.

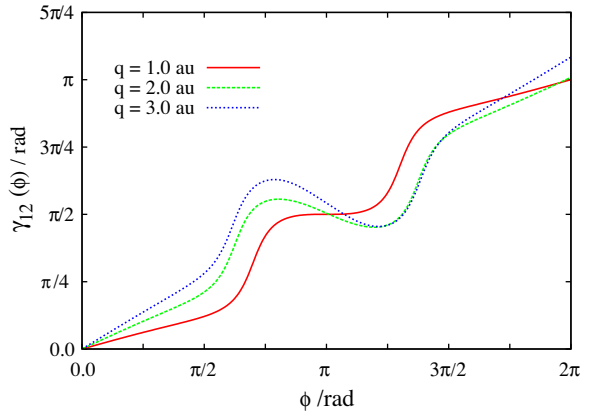

Figure 3. Adiabatic-to-diabatic-transformation (mixing) angle, $\gamma_{12}(\varphi|q)$, for three circular contours at $R = R_{ce} = 6$ au along the interval $0 \leqslant \varphi \leqslant 2\pi$ as calculated employing Eq. (1).

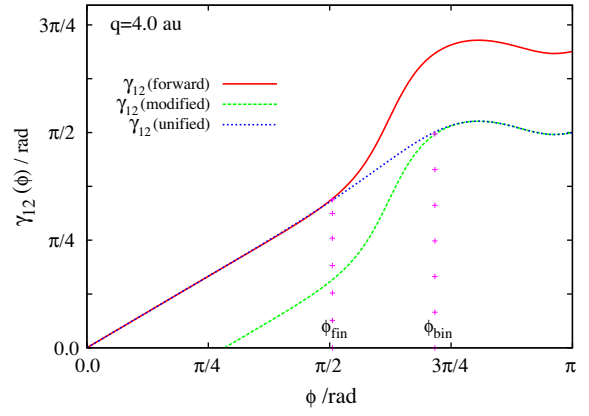

Figure 4. Adiabatic-to-diabatic-transformation (mixing) angle $\gamma_{12}(\varphi|q)$ at $R = R_{ce} = 6$ au, for circular contours ($q = 4$ au) along the interval $0 \leqslant \varphi \leqslant \pi$: The first curve, $\gamma_{12}^{(f)}(\phi|q)$, (—) is calculated employing Eq. (1) in the forward direction; the second curve $\gamma_{12}^{(m)}(\phi|q)$, (- - - -) is calculated employing Eq. (1) in the backward direction (thus forming $\gamma_{12}^{(b)}(\phi|q)$), and then, farther, employing Eq. (I.1) to form the modified curve; the third curve (. . . .) – the unified curve – is formed by merging $\gamma_{12}^{(f)}(\phi|q)$ and $\gamma_{12}^{(m)}(\phi|q)$, and interpolating along the intermediate interval $[\varphi_{fin} \leqslant \varphi \leqslant \varphi_{bin}]$ employing a Least-Square technique.

seam along the collinear HHF axis [25,32]. This effect was recently studied theoretically – a study accompanied with numerical results – and soon will be published [39].

In Figure 3 are presented the ADT angles, $\gamma_{12}(\varphi|q)$, for three radii $q = 1.0$, 2.0, 3.0 au as calculated employing Eq. (1). The expected values of the end-of-the-closed-contour angles (i.e. Berry phases), $\alpha_{12}(q)$ $\{=\gamma_{12}(\varphi = 2\pi|q)\}$ are π and indeed these expectations are fulfilled reasonably well for $q = 1.0$,2.0 au but hardly for $q = 3.0$. In order to correct for this mishap we devised method that applies two line integrals (see Appendix A). The results can be seen in Figure 4.

In Figure 5 are presented comparisons between the original adiabatic PESs, $u_j(R|\theta)$; $j = 1,2$ and the corresponding diabatic PESs

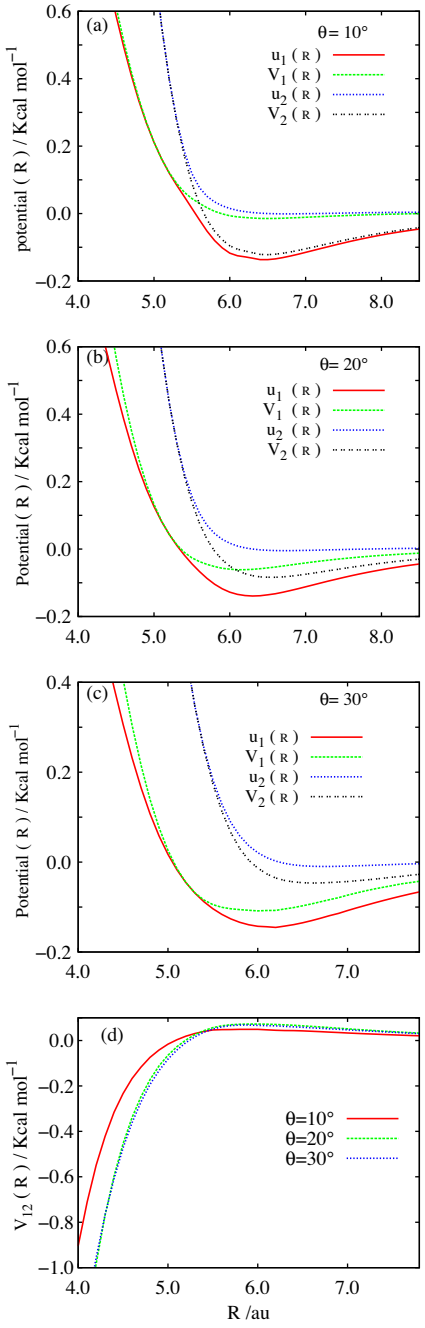

Figure 5. Adiabatic ($u_j(R|\theta)$); $j = 1,2$) and diabatic ($V_j(R|\theta)$; $j = 1,2$) potential energy curves and diabatic coupling terms $V_{12}(R|\theta)$; along polar radii for three fixed polar angles: $\theta = (10°, 20°, 30°)$.

$V_j(R|\theta)$; $j = 1,2$ as a function of R for three values of θ, namely $\theta = \{10°, 20°, 30°\}$ (see panels (a–c), respectively). It is well known that in contrast to the adiabatic PESs one can form numerous sets of diabatic potential all appropriate for deriving the correct probabilities and cross sections. However from the numerical point of view it is always preferred to have *diabatic* potentials which are as close as possible to the *adiabatic* potentials (and therefore diabatic *coupling* terms are as small as possible). Without going into too much detail it is noticed that the present approach yields, from this point of view, a *friendly* set of diabatic potentials.

In addition are shown also, in panel (d), the corresponding diabatic coupling terms, $V_{12}(R|\theta)$. It is well noticed that $V_{12}(R|\theta)$ increases relatively fast as R approaches the center of the coordinates (namely decreases to zero). This increase is directly associated with the corresponding increase of the upper adiabatic PES, $u_2(R|\theta)$.

The main reason for showing the potential curves along the intermediate interval, namely, $R \sim \{4–7\}$ au is to present the intersection region between the two diabatic potentials. In this respect we mention again that the *ci*-point is on the collinear axis at $R \sim 5.5$ au. It is noticed that for the $\theta = 10°$ arrangement the intersection point of the two corresponding diabatic potentials, $V_1(R, \theta = 10°)$ and $V_2(R, \theta = 10°)$, is the closest to the *ci*-point and as the angle θ increases the intersection point moves further and further away from the *ci*-point.

In Figure 6 are presented the equi-potential lines for the two lower PESs, namely, $u_1(R, \theta|r = 1.6$ au) and $V_1(R, \theta|r = 1.6$ au) for the following region: $\{3 \leqslant R \leqslant 8$ au, $0 \leqslant \theta \leqslant 40°\}$. It is seen that the two differ significantly from each other: Whereas the adiabatic potential, $u_1(R, \theta)$, is characterized by one single peak (which occurs at a point on the collinear axis) the diabatic potential, $V_1(R, \theta)$, possesses two symmetric peaks at about $(R, \theta) \cong (\sim 3.9$ au, $\pm 22°)$. Moreover, $V_1(R, \theta)$ shows a typical saddle picture with the mini/max point located at the collinear axis at $R \sim 4$ au. At this stage we need to emphasize that the saddle structure of $V_1(R, \theta)$ is formed for a straight line (along R) and an orthogonal *angular coordinate* and not for two orthogonal straight lines (such as R and r) as are encountered in collinear arrangements.

So far we presented only a small fraction of what was really done. Applying our approach we derived diabatic potentials for nine additional vibrational grid points:

$$r = 0.9,\ 1.0,\ 1.1,\ 1.2,\ 1.3,\ 1.4,\ 1.5,\ (1.6),\ 1.8,\ 2.0 \text{ au}.$$

In all cases accurate (namely, well-converged) calculations were carried out for the same region: $\{3 \leqslant R \leqslant 8$ au, $0 \leqslant \theta \leqslant 40°\}$. The extension to larger θ-values was also done but by less accurate means (namely, applying extrapolation as will be discussed in later publications).

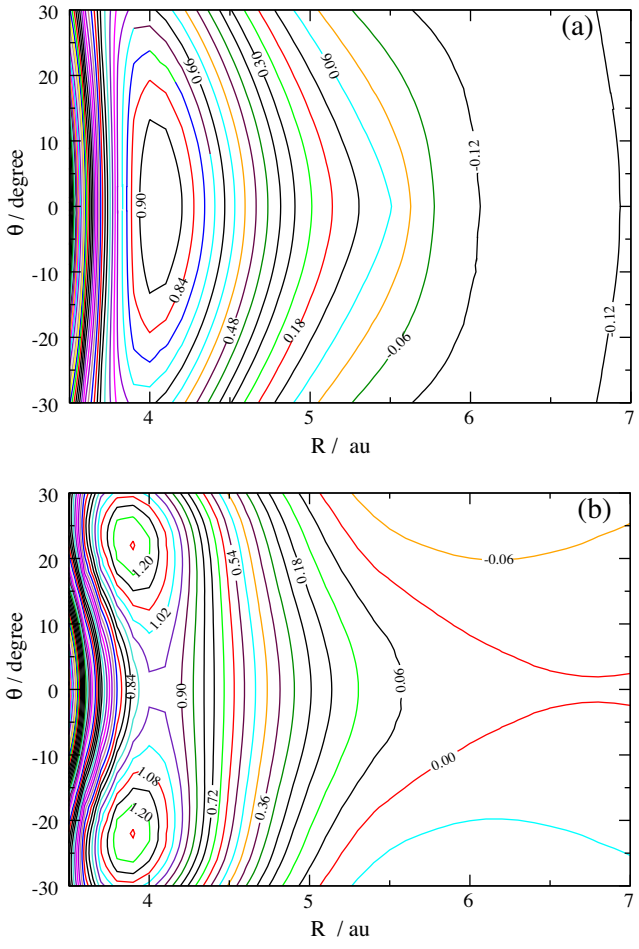

Figure 6. The equi-potential lines of the two lower potentials, namely, $u_1(R, \theta)$ and $V_1(R, \theta)$, emphasizing the differences of their barrier structure (see text). Contours are drawn in steps of 0.06 kcal/mol. In (a) is presented lower *adiabatic* potential, $u_1(R, \theta)$ and in (b) is presented the lower *diabatic* potential, $V_1(R, \theta)$.

4. Conclusions and summary

The present publication differs from other written during the last decade because here for the first time is produced the complete 2×2 single-valued diabatic potential matrix (based on NACTs) that covers, continuously, a sizable region of configuration space. For most parts of this region it was enough to apply the line integral (see Eq. (1)) in order to derive the ADT (mixing) angles that will end up with *quantized* end-of-the-contour ADT angles (i.e. *integer* Berry phases [22]) for the various closed contours. However we also mention that frequently applying the ordinary line integral failed to deliver the required quantization so that we had to use a modified procedure based on two line integrals (see Appendix A).

As was mentioned earlier the $F + H_2$ reaction is one of the more studied reactions and it is somewhat of a surprise that hardly any efforts were made to study the details of its electronic structure, namely, the position of its various *ci*-points (except for the (1,2) *ci* as reported in Ref. [6]) and the shape of the corresponding NACTs, not to mention its corresponding accurate *single-valued* diabatic PESs. Consequently most of the dynamic treatments were carried out employing only the lowest *adiabatic* PES. Surprisingly, these calculations yield results that fit very nicely numerous *types* of experimental measurements ranging from temperature dependent rate constants to energy dependent state-to-state differential cross sections. These facts imply that the reactive $F + H_2$ system can be studied reliably well within the BO *approximation* although its potentials are affected, at critical regions, by a (1,2) JT-*ci*.

In the Section 1 we presented the motivation for our present numerical study. Our aim is to find out whether low energy processes (e.g. *cold* reactions) could also be treated reliably within the BO approximation. To give a meaningful answer we need first to compare certain features that characterize the various potentials that dominate this system and then, at a later stage, perform the dynamics. To fulfill the first stage we need diabatic potentials based on (BO) NACTs. Such *diabatic* potentials were never produced for this system.

In fact Werner et al. [6,18,19] calculated diabatic potentials but instead of employing BO NACTs to form the mixing angles they were derived by analyzing the coefficients in the configuration interaction expansion of the FH_2 wave function. However applying this procedure one is expected to face difficulties concerning the single-valuedness of the diabatic potentials in various regions of

interest because the corresponding Berry phases are not necessarily integers (this issue was raised also in other publications. e.g. [36,37]).

In this respect we mention that we carried out a brief comparison study between the two lowest diabatic potentials, as calculated by applying the two approaches (for instance we compared our equi-potential lines as calculated for $\theta \sim 53^\circ$ with those presented in Fig. 2 of Ref. [19]). We get that in general the equi-potential lines are quite similar but then, sometimes, also differ significantly. For instance we find that the intersection point between the two diabatic potentials $V_1(R,\theta|r)$ and $V_2(R,\theta|r)$ for $r = 1.4$ au and $R = 5.7$ au happens at $\theta \sim 23^\circ$ when Werner's approach is applied (see Fig. 4 in Ref. [6]) and at $\theta \sim 20^\circ$ when NACTs are used (a detailed study for $r = 1.4$ au will soon be presented elsewhere).

As a last issue we refer to the question in what way having consistent PESs (namely fully derived within the BO treatment) is going to affect our understanding of the present, as well as other, reactive processes. In general accurate potentials are always important but we expect the consistent ones (which, of course, have to include the SO coupling) to yield an unambiguous description of the reactive process in the *very low* energy regime where even negligible details of the potential may have a significant effect. We may encounter difficulties in treating a general case but we anticipate that our methodology can be at least applied in those cases where exchange *arrangements-channels* can be safely eliminated by employing *absorbing boundary conditions* [7,16].

Next we summarize the following achievements:

(1) We discussed to some extent the two lowest *ci*s, of this system, namely, the JT (1,2) *ci* and the RT (2,3) *ci* and studied the (1,2) NACTs along closed contours surrounding the (1,2) *ci*.
(2) We report on diabatic potentials calculated for a planar configuration space characterized by r(HH) = 1.6 au (in Fig. 6b are presented equi-potential lines for $V_1(R,\theta)$ for the corresponding planar grid). Similar calculations were carried out for nine more planar grids as detailed in Section 3. These diabatic potentials, given at ten planar grids, form the diabatic potentials for the F + H_2 system on a three dimensional grid.
(3) We emphasize again that during the whole numerical treatment attention was given to guarantee the *single-valuedness* of the reported diabatic potentials on each planar grid.

Acknowledgment

A.D. acknowledges CSIR, India for research fellowship, D.M. and S.A. acknowledge the BRNS, India for Grants (sanction No. 2009/37/42/BRNS) in computational facilities.

Appendix A

A.1. Derivation of the complementary line integral

As mentioned in the Letter we find that for the larger (circular) contours ($q \geqslant 3$ au) the line integral (in Eq. (1)) does not yield the expected integer Berry-phases. In such a case we usually consider more states (namely solve line integrals for NACT *matrices* and in this way overcome this difficulty [41]. In our present case considering a 3×3 matrix is not feasible as the second NACT is a singular RT NACT which numerically may cause difficulties. Consequently we developed a new methodology to calculate a mixing angle with the correct Berry phases.

This treatment is based on the fact that the HHF system is *symmetric* with respect to the collinear axis (see Fig. 1). Consequently we get, for any circular contour with its center located on the collinear axis, that $\gamma_{12}(\varphi = 2\pi|q) = 2\gamma_{12}(\varphi = \pi|q)$. However, since we demand that for a full circle: $\gamma_{12}(\varphi = 2\pi|q) = \pi$ we should get for half a circle, $\{0,\pi\}$: $\gamma_{12}(\varphi = \pi|q) = \pi/2$. Having established this result the idea is to carry out the line integral (see Eq. (1)) two times – each time with a different initial point:

(a) Integrating forward (the ordinary way), starting at $\varphi = 0$ and ending at some intermediate value $\varphi = \varphi_{\text{fin}}$ (see Fig 4) thus yielding $\gamma_{12}(\varphi|q) = \gamma_{12}^{(\text{f})}(\phi|q)$ along the interval $0 \leqslant \varphi \leqslant \varphi_{\text{fin}}$. Here 'f' stands for *forward*.
(b) Integrating backward, namely, starting at $\varphi = \pi$ and ending at $\varphi = \varphi_{\text{bin}}$ thus yielding $\gamma_{12}^{(\text{b})}(\phi|q)$ for the interval $\varphi_{\text{bin}} \leqslant \varphi \leqslant \pi$ (see Fig. 4). Here 'b' stands for *backward*.

It can be shown that having $\gamma_{12}^{(\text{b})}(\phi|q)$ we are able to form the modified part of the (ill-conditioned) $\gamma_{12}(\varphi|q)$, (along the interval $\varphi_{\text{bin}} \leqslant \varphi \leqslant \pi$), by making the simple connection:

$$\gamma_{12}^{(\text{m})}(\phi\ \text{q}) = \pi/2 - \gamma_{12}^{(\text{b})}(\phi\ \text{q}) \tag{I.1}$$

Here '*m*' stands for *modified*.

A.2. Explanation

According to the procedure just described, $\gamma_{12}^{(\text{f})}(\phi|q)$ is expected to be accurate for the lower φ-interval, namely, in the vicinity of $\varphi \sim 0$ and up to some value $\varphi = \varphi_{\text{fin}}$ whereas $\gamma_{12}^{(\text{m})}(\phi|q)$ is expected to be accurate for the upper φ-interval in the vicinity of $\varphi \sim \pi$ and down to some value $\varphi = \varphi_{\text{bin}}$ (see Fig. 4). To get the full (physical) curve $\gamma_{12}^{(\text{u})}(\phi|q)$ – where u stands for 'unified' – for the interval of interest, $0 \leqslant \varphi \leqslant \pi$, we *interpolate* along the intermediate region $\varphi_{\text{fin}} \leqslant \varphi \leqslant \varphi_{\text{bin}}$ so that the two curves, $\gamma_{12}^{(\text{f})}(\phi|q)$ and $\gamma_{12}^{(\text{m})}(\phi|q)$, from left and right, respectively, merge *smoothly* to form one single curve. This single curve (in Fig. 4) is formed applying the Least Square method which is based on the given values of $\gamma_{12}^{(\text{f})}(\phi|q)$ and $\gamma_{12}^{(\text{m})}(\phi|q)$ along the corresponding intervals: $0 \leqslant \varphi \leqslant \varphi_{\text{fin}}$ and $\varphi_{\text{bin}} \leqslant \varphi \leqslant \pi$.

Appendix B

B.1. The numerical treatment

Adiabatic potential energy surfaces of the two lowest adiabatic states, $1\ ^2A'$ and $2\ ^2A'$ have been generated at MRCI level added with Davidson correction [42] using MOLPRO program [40]. The active space has been chosen as comprising of the 3σ-6σ orbitals, 1π valence orbitals and one additional set of correlating 2π orbitals. Care has been taken [6] to avoid the swap of 2σ and 3σ orbitals during the optimization of the orbitals at the CASSCF level. The basis set employed are: For the fluorine we applied s and p functions from the cc-pV5Z set and d, f and g functions from cc-pVQZ set augmented with diffuse s, p, d, f and g functions. For the hydrogens we employed s functions from the cc-pV5Z set and p and d functions from the cc-pVQZ set augmented with diffuse s and p functions. The calculation of the non-adiabatic coupling terms (along chosen circles) was carried out at the state-average CASSCF level using the MOLPRO program [40], employing the above basis without the g functions. In this calculation we used the active space including all seven valence electrons distributed on eight (8) orbitals. Six electronic states, including the two studied states, were computed by the state-average CASSCF method with equal weights.

References

[1] T.P. Shafer, P.E. Siska, J.M. Marson, F.P. Tully, Y.C. Wong, Y.T. Lee, J. Chem. Phys. 53 (1970) 3385.
[2] J.C. Polanyi, S. Woodall, J. Chem. Phys. 57 (1972) 1575.
[3] M. Baer, M. Faubel, B. Martin'ez-Haya, L.Y. Rusin, U. Tapp, J.P. Toennies, J. Chem. Phys. 108 (1998) 9694.
[4] G.C. Schatz, J.M. Bowman, A. Kuppermann, J. Chem. Phys. 56 (1973) 1024.
[5] J. Jellinek, M. Baer, D.J. Kouri, Phys. Rev. Lett. 47 (1981) 1588.
[6] K. Stark, H.-J. Werner, J. Chem. Phys. 104 (1996) 6515.
[7] E. Rosenman, Z. Hochman-Kowal, A. Persky, M. Baer, Chem. Phys. Lett. 257 (1996) 421.
[8] D.E. Manolopoulos, Chem. Soc. 93 (1997) 673.
[9] F.J. Aoiz, L. Banares, F. Castillo, J. Chem. Phys. 111 (1999) 4013.
[10] B. Martinez-Haya, F.J. Aoiz, L. Banares, P. Honvault, J.M. Launay, Phys. Chem. Chem. Phys. 1 (1999) 3415.
[11] V. Aquilanti, S. Cavalli, D. De Fazio, A. Volpi, A. Aguilar, J. Maria Lucas, Chem. Phys. 308 (2005) 237.
[12] E. Bodo, F.A. Gianturco, A. Dalgarno, J. Chem. Phys. 116 (2002) 9222.
[13] N. Balakrishnan, A. Dalgarno, J. Phys. Chem. A 107 (2003) 7101.
[14] R.V. Krems, Int. Rev. Phys. Chem. 24 (2005) 99.
[15] P.F. Weck, Balakrishnan, Int. Rev. Phys. Chem. 25 (2006) 283.
[16] S. Bovino, M. Taccomi, F.A. Gianturco, J. Phys. Chem. A 115 (2011) 8197.
[17] S.H. Lipoff, D. Herschbach, Mol. Phys. 108 (2010) 1133.
[18] M.H. Alexander, H.-J. Werner, D.E. Manolopoulos, J. Chem. Phys. 109 (1998) 5710.
[19] M.H. Alexander, D.E. Manolopoulos, H.-J. Werner, J. Chem. Phys. 113 (2000) 11084.
[20] M. Baer, Beyond Born Oppenheimer; Electronic non-Adiabatic coupling Terms and Conical Intersections, Wiley & Sons Inc., Hoboken N.J., 2006.
[21] M. Baer, Chem. Phys. Lett. 35 (1975) 112.
[22] M.V. Berry, Proc. Roy. Soc. Lond. A 392 (1984) 45.
[23] A. Alijah, M. Baer, J. Phys. Chem. A 104 (2000) 389.
[24] T. Ve'rtesi, Á. Vibók, G.J. Halász, M. Baer, J. Phys. B: At., Mol. Opt. Phys. 37 (2004) 4603.
[25] A. Das, D. Mukhopadhyay, S. Adhikari, M. Baer, J. Chem. Phys. 133 (2010) 084107.
[26] Ref. 20, Sect. 3.1.1.3.
[27] M. Baer, Adv. Chem. Phys. 49 (1982) 191 (see p. 283).
[28] Z.H. Top, M. Baer, Chem. Phys. 25 (1977) 1.
[29] T.C. Thompson, D.G. Truhlar, C.A. Mead, J. Chem. Phys. 82 (1985) 2392.
[30] G.J. Halász, Á. Vibók, A.M. Mebel, M. Baer, Chem. Phys. Lett. 358 (2002) 163 (see Fig. 1).
[31] S. Han, D. Yarkony, J. Chem. Phys. 119 (2003) 5058.
[32] G.J. Halász, Á. Vibók, R. Baer, M. Baer, J. Chem. Phys. 125 (2006) 094102.
[33] S. Al-Jabour, M. Baer, O. Deeb, M. Liebscher, J. Manz, X. Xu, S. Zilberg, J. Phys. Chem. A 114 (2010) 2991.
[34] M.S. Kaczmarski, Y. Ma, M. Rohlfing, Phys. Rev. B 81 (2010) 115433.
[35] A. Sirjoosingh, S. Hammes-Schiffer, J. Phys. Chem. A 115 (2011) 2367.
[36] W. Skomorowski, F. Pawlowski, T. Korona, R. Moszinski, P.S. Zuckowski, J.M. Hutson, J. Chem. Phys. 134 (2011) 114109.
[37] M.S. Kaczmarski, M. Rohlfing, J. Phys. B: At., Mol. Phys. 43 (2010) 051001.
[38] A. Yahalom, Advances in Classical Field Theory, Bentham eBooks eISBN: 978-1-60805-195-3, 2011 (Chapter 9).
[39] A. Das, D. Mukhopadhyay, S. Adhikari, M. Baer, Int. J. Quant. Chem., in press.
[40] MOLPRO is a package of *ab initio* programs written by H-J. Werner, P. J. Knowles, with contributions from J. Almlöf, et al.
[41] M. Baer, Mol. Phys. 40 (1980) 1011.
[42] S.R. Langhoff, E.R. Davidson, Int. J. Quant. Chem. 8 (1974) 61.